Impurity scattering and transport of fractional quantum Hall edge states

C.L. Kane
Department of Physics, University of Pennsylvania, Philadelphia, Pennsylvania 19104

Matthew P.A. Fisher
Institute for Theoretical Physics, University of California, Santa Barbara, Santa Barbara, California 93106
(Received 7 September 1994)

We study the effects of impurity scattering on the low-energy edge-state dynamics for a broad class of quantum Hall fluids at filling factor $\nu = n/(np+1)$, for integer n and even integer p. When p is positive all n of the edge modes are expected to move in the same direction, whereas for negative p one mode moves in a direction opposite to the other $n-1$ modes. Using a chiral-Luttinger model to describe the edge channels, we show that for an ideal edge when p is negative, a nonquantized and nonuniversal Hall conductance is predicted. The nonquantized conductance is associated with an absence of equilibration between the n edge channels. To explain the robust experimental Hall quantization, it is thus necessary to incorporate impurity scattering into the model, to allow for edge equilibration. A perturbative analysis reveals that edge impurity scattering is relevant and will modify the low-energy edge dynamics. We describe a nonperturbative solution for the random n-channel edge, which reveals the existence of a disorder-dominated phase, characterized by a stable zero-temperature renormalization-group fixed point. The phase consists of a single propagating charge mode, which gives a quantized Hall conductance, and $n-1$ neutral modes. The neutral modes all propagate at the same speed, and manifest an exact SU(n) symmetry. At finite temperatures the SU(n) symmetry is broken and the neutral modes decay with a finite rate which varies as T^2 at low temperatures. Various experimental predictions and implications which follow from the exact solution are described in detail, focusing on tunneling experiments through point contacts.

I. INTRODUCTION

It was over a quarter of a century ago that pioneering theoretical work on one-dimensional interacting electron gases demonstrated the profound effects that electron-electron interactions can have in low-dimensional quantum systems.[1–3] Specifically, it was found that even weak repulsive interactions destablize a Fermi-liquid description of a one-dimensional electron gas. Some years later,[4] Haldane coined the term "Luttinger liquid" to describe the generic state of a one-dimensional interacting electron gas. Since then it has become possible to fabricate one-dimensional electron gases in semiconductors,[5,6] by clever lithography on semiconductor heterostructures. Unfortunately, searches for non-Fermi-liquid properties in such one-dimensional quantum wires has been impeded by spurious impurities,[7] which tend to localize the electrons. It has recently been emphasized,[8–11] though, that the quantum Hall effect might serve as an alternate arena to study one-dimensional electron gases. In the presence of a strong external magnetic field, a two-dimensional electron gas forms an incompressible quantum Hall fluid[12] and the current that flows is confined to the edges. These current carrying edge states provide a unique laboratory for the study of "ideal" one-dimensional systems.

Indeed, a key feature of quantum Hall edge states is their resilience in the presence of disorder.[13] For example, electrons on the edge of a quantum Hall state at filling factor $\nu = 1$, which corresponds to a full Landau level, are completely insensitive to the presence of disorder on the edge. This is because edge-state electrons propagate in only one direction, and hence cannot be backscattered by random impurities. There is no localization, and the only effect of disorder is to give the electrons an unimportant forward scattering phase shift. In fact, the very quantization of the Hall conductance in the integer effect can be understood simply in the framework of the Landauer-Buttiker theory,[14] which relates the quantized conductance to the perfect transmission of free-electron edge states.

When there are multiple edge channels, such as for the integer quantum Hall effect at n full Landau levels, $\nu = n$, disorder plays a more important role by causing the scattering of electrons between the different channels.[15] However, in this case the channels all propagate in the same direction, so that, as indicated in Fig. 1(a), the net current is not altered by the scattering events. The total transmission and resulting conductance is still quantized. Nonetheless, it has been possible to probe such inter-channel scattering by selectively "feeding" different edge modes from contacts at different chemical potentials, and then examining the resulting equilibration.[16,17]

In the fractional quantum Hall effect, the free-electron edge-state theories can no longer be applied. Recently, however, an alternative description has been proposed by Wen[9] in which the edge states in the fractional quantum Hall effect are described by a chiral-Luttinger liquid

0163-1829/95/51(19)/13449(18)/$06.00

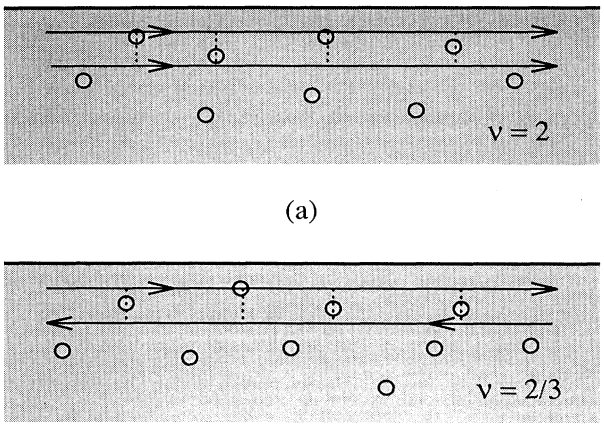

FIG. 1. Schematic portrait of the edge of a quantum Hall state with two channels. The presence of random impurities, denoted by the small circles, allows for momentum nonconserving scattering between the different channels. When the channels move in the same direction (e.g., $\nu = 2$), as shown in (a), interchannel scattering does not effect the net transmission of the edge. However, when the channels move in opposite directions, as in $\nu = 2/3$, depicted in (b), the backscattering of charge plays a crucial role.

model. In particular, for the Laughlin states, such as $\nu = 1/3$, the edge states consist of a single branch, and are described by a single-channel chiral-Luttinger liquid. As in the case of $\nu = 1$, edge disorder is expected to play no role in these states. Recent experiments on tunneling between edge states at a point contact in the $\nu = 1/3$ quantum Hall effect support the chiral-Luttinger liquid model.[18]

For hierarchical quantum Hall states, there will be many branches of edge excitations.[9] In general, at the nth level of the Haldane-Halperin hierarchy,[19] the appropriate description is an n-channel chiral-Luttinger liquid. In Wen's theory, the universal properties of the bulk Hall fluid determine the direction of propagations of the edge modes. In contrast to the integer quantum Hall effect, there is a class of fractional Hall states for which the n edge modes are not all moving in the same direction.[9,10] Unfortunately, as we show in detail below, in these cases the theory predicts a value of the conductance which is not correctly quantized, depending on nonuniversal interaction parameters at the edge.

In a recent paper with Polchinski,[20] we argued that for this class of fractional Hall states it is absolutely crucial to include impurity scattering at the edge. Such scattering allows for charge transfer between channels moving in opposite directions, as shown in Fig. 1(a), and can modify the conductance. Specifically, we studied the effects of such interchannel impurity scattering at the edge of a $\nu = 2/3$ quantum Hall state.[20] In the absence of impurities, the simplest model[9,10] of a $\nu = 2/3$ edge consists of two charged modes: one with conductance e^2/h and another with conductance $(1/3)e^2/h$, which moves in the opposite direction. We found that even weak interchannel impurity scattering is relevant, and at low energies the edge is described by a new disorder dominated phase. An exact solution in this phase revealed the presence of a single charged mode, which gave the correct quantized conductance of $2/3(e^2/h)$, and a neutral mode which propagates in the opposite direction. The neutral mode was shown to possess an exact SU(2) symmetry.

In this article we elaborate significantly on the above results and generalize them to fractional quantum Hall states at higher levels of the hierarchy. Specifically, we consider quantum Hall states at filling factors $\nu = n/(np+1)$, with p an even integer and n an arbitrary positive integer. Within Jain's hierarchical construction,[21] these states can be achieved by attaching flux tubes with p flux quanta to each electron, and putting the resulting composite fermions in n full Landau levels. With this convention, p can be a negative even integer, in which case the filling factor is $-\nu$. For this broad class of quantum Hall fluids, we find the presence of edge impurity scattering drives the edge modes to a new fixed point in which the charge and neutral sectors decouple at low energies. More specifically, the edge fixed point is characterized by a single propagating charged mode with conductance $|\nu|e^2/h$ and $n-1$ neutral modes. The $n-1$ neutral modes will be shown to have an exact SU(n) symmetry, implying that they all move at the same velocity. The direction of propagations of the neutral modes with respect to the charge mode is determined by the sign of p, moving in a direction opposite to the charge mode for p negative.

Since our initial Hamiltonian for the edge modes has only one conserved U(1) charge, the physical electric charge, the presence of the additional $n-1$ propagating neutral modes is quite surprising. However, the fixed point to which the system scales at low energies has much higher symmetry — an exact U(1)×SU(n) symmetry— than the original Hamiltonian. Indeed, it is the presence of the SU(n) symmetry at the attractive fixed point that leads to the existence of the $n-1$ additional neutral modes.

Since the fixed point is a zero-temperature fixed point, the SU(n) symmetry is broken at finite temperatures. It follows that at $T \neq 0$ the neutral modes are not conserved and will decay with a lifetime τ_σ, or equivalently a finite decay length $\ell_\sigma = v_\sigma \tau_\sigma$, where v_σ is the velocity of the neutral modes. By analyzing the leading irrelevant operators, which control the flows into the zero-temperature fixed point, we will show that the decay rate vanishes algebraically at zero temperature:

$$\frac{1}{\tau_\sigma} \propto T^2. \tag{1.1}$$

In contrast, the charge mode cannot decay, even at finite temperature, since electric charge is always conserved. However, due to irrelevant operators, which couple the charge and neutral sectors, the charge mode can scatter off the neutral modes. This leads to a charge mode that propagates with a dispersion $\omega = v_\rho q + iDq^2$, with a "diffusion" constant D, which is temperature independent at low-temperatures. This implies a diffusive spreading of a

charge pulse as it propagates along an edge.

On length scales longer than ℓ_σ, it is appropriate to adopt a "hydrodynamic" description of the edge propagation, in which there is only a single propagating mode associated with the conserved electric charge. However, this hydrodynamic picture leaves out important low-temperature physics, which can be accessed via interedge tunneling. We shall return to this point in Sec. IV.

The existence of an attractive zero-temperature fixed point with higher symmetry than the underlying Hamiltonian is reminiscent of Fermi-liquid theory. The zero-temperature Fermi-liquid fixed point has, in addition to conserved electric charge, an infinity of conserved charges [and hence an infinity of U(1) symmetries] associated with each point on the Fermi surface. This is the symmetry responsible for the quasiparticle excitations. At finite temperatures, this symmetry is broken, leading to a finite scattering lifetime for the quasiparticles, proportional to T^{-2}. Since the total electric charge is conserved, there remains a propagating zero sound mode in a Fermi liquid, which does not decay. It is amusing that we find a scattering rate for the neutral edge excitations, Eq. (1.1), which vanishes with the same power of temperature—T^2—as the quasiparticles in a Fermi liquid.

At low temperatures, the restoration of the full SU(n) symmetry at the edge of a random $\nu = n/(np+1)$ Hall state has important experimental consequences. When p is negative, and the neutral modes travel in the opposite direction to the charge mode, the very quantization of the Hall conductance rests on this symmetry. As we show explicitly below, in the absence of edge randomness which equilibrates the edge modes, a nonuniversal value of the Hall conductance is predicted[20] for $p < 0$.

The presence of the SU(n) edge symmetry also implies universal values for the scaling dimensions of the edge tunneling operators. These scaling dimensions are experimentally accessible, by measuring the temperature dependence of the tunneling conductance through a point contact.[18,11,26] Our central prediction is that when p is negative, the conductance through a point contact in a $\nu = n/(np+1)$ Hall fluid should vanish as

$$G(T) \propto T^{\alpha}, \tag{1.2}$$

where

$$\alpha = 2|p| - (4/n). \tag{1.3}$$

For the $p = -2$ sequence, the predicted exponents are displayed in Table I. The exponents approach $\alpha = 4$ as ν approaches $1/2$. For non-negative p, an exponent $\alpha = 2p$ is predicted.

A measurement of temperature exponents consistent with these would give indirect evidence of the neutral modes, since the electron that tunnels through the point contact is "built" from a superposition of the charge and neutral edge modes. The neutral modes should be measurable more directly, though, via time domain experiments, which we discuss below. In this way, one might be able to measure directly the temperature-dependent decay rate of the neutral mode—roughly analogous to a direct measurement of a decaying Fermi-liquid quasiparticle.

TABLE I. Tunneling exponent α for the temperature-dependent conductance (1.2) through a point contact separating two quantum Hall fluids at filling factor ν.

ν	1/3	2/5	3/7	4/9
α	4	4	4	4
ν	2/3	3/5	4/7	5/9
α	2	8/3	3	31/5

The outline of our paper is as follows. In Sec. II, we describe the model for an impurity free quantum Hall edge at filling $\nu = n(np+1)$, which consists of an n-channel chiral-Luttinger liquid. We split the model into two pieces, denoted S_0 and S_1, and show that the first piece can be conveniently decoupled into a charge sector and a neutral sector with $n-1$ modes. We then demonstrate that S_0 possesses an exact U(1)×SU(n) symmetry. This symmetry is not respected by S_1, however. In Sec. III, we consider the addition of the most general random impurity scattering terms. Although these random terms break the U(1)×SU(n) symmetry of S_0, we show in Sec. III A that provided S_1 is ignored the random model can be solved exactly. In terms of new fields, the exact solution reveals an exact U(1)×SU(n) symmetry. In Sec. III B we show that the exact solution is perturbatively stable in the presence of nonzero S_1. The effects of small nonzero temperatures are considered in Sec. III C. In Sec. IV, we use the exact solution of the random edge to calculate the scaling dimension of edge tunneling operators, which are relevant to experiments on tunneling through a point contact. Section V is devoted to specific experimental predictions, and a more general discussion of our central results.

II. THE CLEAN EDGE

A. The model

The topological order of a quantum Hall state in the nth level of the hierarchy is characterized by a symmetric $n \times n$ matrix K. The low-energy physics of a hierarchical quantum Hall state may be described by n gauge fields with an effective action,[22,23]

$$S_{\rm bulk} = \frac{i}{4\pi} \int a^i_\mu K_{ij} \epsilon_{\mu\nu\lambda} \partial_\nu a^j_\lambda. \tag{2.1}$$

We use the "symmetric" basis in which the electron three-current is given by

$$j_\mu = \sum_i \epsilon_{\mu\nu\lambda} \partial_\nu a^i_\lambda / 2\pi. \tag{2.2}$$

In this basis, the filling factor is given by

$$\nu = \sum_{ij} K^{-1}_{ij}. \tag{2.3}$$

For the quantum Hall states at filling $\nu = n/(np+1)$, in both the Haldane-Halperin hierarchy and in the Jain construction, the K matrix is given explicitly by

$$K_{ij} = \delta_{ij} + p. \tag{2.4}$$

The K matrix characterizes the charge and statistics of the bulk quasiparticle excitations. Specifically, the quasiparticles are labeled by a set of integers m_j, with $j = 1, 2, \ldots, n$, and in the symmetric basis have a charge (in units of the electron charge)

$$Q = \sum_{ij} m_i K^{-1}_{ij} \tag{2.5}$$

and statistics angle

$$\frac{\Theta}{\pi} = \sum_{ij} m_i K^{-1}_{ij} m_j. \tag{2.6}$$

In this approach, all of the universal properties of the bulk quantum Hall state follow directly from the K matrix.

It is worth emphasizing the implicit assumptions that were needed to arrive at the simple form (2.1). These can be perhaps most easily understood in terms of the Ginzburg-Landau description[24] of the Hall effect. For $\nu = n/m$ with m odd, n electrons bind with m vortices forming a "molecule" with bosonic statistics. At the magic rational filling factor $\nu = n/m$, all of the vortices induced by the magnetic field are accommodated in this way. The electron/vortex composites can then Bose condense, leading to the quantum Hall effect. The effective action (2.1) describes the long wavelength density fluctuations of this condensed fluid. The bulk quasiparticle excitations, referred to above, are essentially excitations involving breaking apart the electron/vortex composites. Although the K matrix determines the charge and statistics of these quasiparticles, the energy gap for their creation is not specified by the effective action (2.1). Provided the temperature is well below these energy gaps, the effective action (2.1) provides an adequate description. However, at filling factors away from $\nu = n/m$, there will be some residual vortices, and the electron/vortex composites can only condense if these residual vortices are pinned and localized by bulk impurities. In this case, there will be many low energy, but spatially localized, excitations involving rearranging the positions of these vortices. The effective action (2.1) can presumably still be used to extract transport properties, though, since at low temperatures the localized vortices will not contribute significantly to the transport. (This is not the case for other physical properties such as the electronic specific heat.) Although the quasiparticle excitations are not important at low T in the bulk, they play a crucial role at the edge. At the edge, their gap vanishes and they form the edge states, which we next discuss.

As shown by Wen,[9] the edge excitations may be described by eliminating the bulk degrees of freedom from (2.1). Upon integration over a^i_τ, a constraint on the density fluctuations in the bulk is imposed: $\vec{\nabla} \times \vec{a}^i = 0$, for all $i = 1, 2, \ldots, n$. Here a vector refers to the two spatial components. Scalar fields can then be introduced to solve these constraints, $\vec{a}^i = \vec{\nabla}\phi_i$, one for each gauge field. The edge excitations are then described in terms of these scalar fields. The appropriate effective action at the edge can then be written as $S = S_0 + S_1$ with

$$S_0 = \int dx d\tau \frac{1}{4\pi}\left[\sum_{ij}(\partial_x\phi_i)K_{ij}(i\partial_\tau\phi_j) + v\sum_i(\partial_x\phi_i)^2\right] \tag{2.7}$$

and

$$S_1 = \int dx d\tau \frac{1}{4\pi}\sum_{ij} V_{ij}\partial_x\phi_i\partial_x\phi_j\ , \tag{2.8}$$

with $\sum_i V_{ii} = 0$. Here x is a one-dimensional spatial coordinate, which runs along the edge, and τ is imaginary time. In addition to the K term, whose form is determined solely from the bulk physics, we also have interaction terms of the form $\partial_x\phi_i\partial_x\phi_j$. These interaction strengths are nonuniversal, and depend on the form of the edge confining potential and the details of the electron-electron interactions (which we assume here to be short ranged, screened by a ground plane). For later convenience, we have split these interaction terms into a constant velocity piece, v in S_0, and a traceless velocity matrix V_{ij} in S_1.

It follows from Eq. (2.2) that the one-dimensional electron charge density along the edge is given by

$$\rho(x) = \frac{1}{2\pi}\sum_{i=1}^{n}\partial_x\phi_i. \tag{2.9}$$

Operators that create charge at the edge can be deduced by noting that the momentum conjugate to the fields is $\Pi_i = (1/2\pi)K_{ij}\partial_x\phi_j$. Thus, an operator of the form $\exp i\phi_i(x)$, which can be expressed as a spatial integral over the conjugate momenta, creates "instantons" in the boson fields ϕ_j at position x. These instantons carry electron charge, as can be seen from (2.9). Specifically, the general edge creation operator

$$\hat{T}(x) = e^{i\sum_{j=1}^{n} m_j\phi_j(x)} \tag{2.10}$$

for arbitrary integers m_j, creates an edge excitation at x with charge Q given in (2.5). Note that the quantum numbers describing the charged edge excitations correspond precisely to the quantum numbers of the bulk quasiparticles.

B. Absence of edge equilibration

The beautiful feature of the effective action (2.7) and (2.8) is it simplicity: It is quadratic in the boson fields, and all physical quantities can thus be easily computed. Unfortunately, when p is negative, the results are in serious conflict with experiment. The most worrisome conflict involves the Hall conductance itself,[20] which we find

is not given by the quantized value $|\nu|e^2/h$.[25]

The difficulty occurs when all of the edge modes do not propagate in the same direction. As shown in Appendix A, the sign of the eigenvalues of the K matrix determines the direction of propagation of the eigenmodes. We show in Sec. II C below that for $\nu = n/(np+1)$ the K matrix has $n-1$ degenerate eigenvalues equal to one, and one eigenvalue equal to $(1+np)$. Thus, when p is negative, there is one mode that moves in a direction opposite to the other $n-1$ modes.

To show that the conductance is nonuniversal for negative p and to gain a physical understanding for why this is, it is useful to generalize the Landauer-Buettiker transport theory to that of an interacting Luttinger liquid. To this end, consider an edge state that flows between two reservoirs, which are in equilibrium at different chemical potentials (see Fig. 2). We model the reservoirs by considering an infinite edge, in which the "sample" resides between x_L and x_R. The left and right reservoirs are then defined for $x < x_L$ and $x > x_R$, respectively. We suppose that the system is driven from equilibrium by an electrostatic potential $eV(x)$, which couples to the edge charge density $\rho(x)$, and is a constant $eV_{L(R)}$ in the left (right) reservoir. The underlying physical assumption of this approach is that the edge states that emanate from a given reservoir are in equilibrium at the chemical potential of that reservoir.

Since the edge current operator is linear in the boson fields,

$$\hat{I}_{\rm edge} = e\frac{1}{2\pi}\sum_{j=1}^{n}\dot{\phi}_j, \tag{2.11}$$

the edge current at a point x which flows in linear response to $V(x')$ may be computed directly. Specifically,

$$I_{\rm edge}(x) = \int dx' D^R(x-x',\omega\to 0)V(x'), \tag{2.12}$$

where the retarded response function is given by

$$D^R(x-x',\omega) = -i\int_{-\infty}^{0} dt e^{-i\omega t}\sum_{i,j}\frac{e^2}{(2\pi)^2\hbar} \times\langle[\dot{\phi}_i(x,0),\partial_{x'}\phi_j(x',t)]\rangle. \tag{2.13}$$

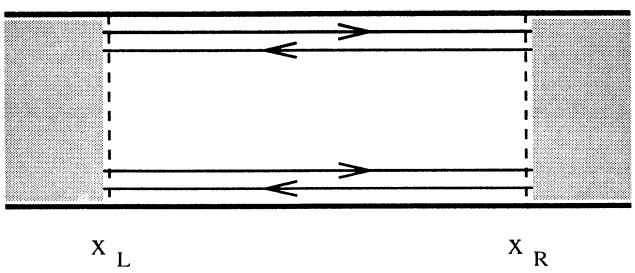

FIG. 2. Schematic diagram of a two-terminal conductance measurement for a quantum Hall state with two channels, which move in opposite directions [i.e., $\nu = 2/(2p+1)$ with $p<0$]. The shaded regions denote the reservoirs.

Consider first the simple case of a single channel edge, such as $\nu = 1/m$, described by the action (2.7) with $K_{11} = \eta m$. Here $\eta = \pm 1$ determines the direction of edge propagation. Using (2.7), the response function (2.13) may be readily computed by analytically continuing the imaginary time response function

$$D(x-x',\omega_n) = -\frac{1}{m}\frac{e^2}{h}\sum_q e^{iq(x-x')}\frac{q\omega_n}{q(\eta i\omega_n - vq)} \tag{2.14}$$

to real frequencies, $i\omega_n \to \omega + i\epsilon$. We then find

$$D^R(x-x',\omega) = \frac{1}{m}\frac{e^2}{h}\theta(\eta(x-x')) \times\frac{i\eta\omega}{v}e^{i\eta(\omega+i\epsilon)(x-x')/v}. \tag{2.15}$$

Note the presence of the θ function, which shows that the current at x depends only on the voltages at positions x' that are "upstream" of x. This reflects the chiral nature of the edge-state propagation. In the limit $\omega \to 0$, the integral in (2.12) will be dominated by values of x' that are deep into the "upstream" reservoir. Thus, for $\eta = +1$, that corresponds to an edge that propagates from left to right, the current is

$$I_{\rm edge} = \frac{1}{m}\frac{e^2}{h}V_L. \tag{2.16}$$

The two-terminal conductance of a Hall bar in the $\nu = 1/m$ state follows if we consider, in addition, the opposite edge, which emanates from the right reservoir and contributes a current $-1/m(e^2/h)V_R$. The net current is thus $I = G(V_L - V_R)$, with an appropriately quantized two-terminal conductance: $G = (1/m)(e^2/h)$.

This approach can easily be generalized to the hierarchical quantum Hall states, which have multiple channels. However, the situation is more complicated if channels on a given edge move in both directions. In Fig. 2, we consider a two-channel example in which the top edge contains two modes, which propagate in opposite directions. Clearly, the current on the top edge will depend on the voltages in both reservoirs. In Appendix A, we show that, in general, the edge current may be written

$$I_{\rm edge} = \frac{e^2}{h}\left(g_+V_L - g_-V_R\right), \tag{2.17}$$

where g_+ (g_-) is the total dimensionless conductance from all right (left) moving channels. When all of the channels move in the same direction either g_+ or g_- will be equal to zero. However, for $p<0$, when channels move in both directions, they will both be positive.

The two-terminal conductance then follows by considering the other edge, which carries a current $g_-V_L - g_+V_R$. Thus, we find

$$G = \frac{e^2}{h}(g_+ + g_-). \tag{2.18}$$

Notice that the conductances of each mode add in parallel, irrespective of their direction of propagation. In Appendix A, we explicitly compute g_+ and g_- using the

effective action (2.7) and (2.8), and show that they are nonuniversal, depending on the interaction strengths V_{ij} in (2.8). However, the combination $g_+ - g_- = \nu$ is shown to be universal. Thus, we see that if all channels move in the same direction, the two-terminal conductance has the quantized value $G = |\nu|e^2/h$. However, when there are channels moving in both directions, the two-terminal conductance will be nonuniversal, and will, in general, be larger than $|\nu|e^2/h$.

It is straightforward to generalize the above approach, based on the right and/or left conductances, $g_\pm$, to compute the conductance measured in a four-terminal geometry. In particular, we find that the four-terminal Hall conductance is given by

$$G_H = \frac{e^2}{h}\frac{g_+^2 + g_-^2}{g_+ - g_-}. \tag{2.19}$$

Thus, it is only when all channels propagate in the same direction that G_H is universal and equal to $\nu e^2/h$.

In Appendix A, we also show that the scaling dimensions of tunneling operators are similarly universal only when all channels move in the same direction. These scaling dimensions enter into experimentally accessible quantities, such as the temperature dependence of tunneling through a point contact. We will discuss this point in more detail in Sec. IV.

We thus see that when p is negative, the Luttinger edge model, (2.7) and (2.8), predicts a two-terminal and Hall conductance that is not quantized, in glaring contradiction with experiment. Clearly some important physics must be absent from the simple effective action (2.7). A clue can be seen from Fig. 2, where it is clear that in a transport situation, right moving edge modes are in equilibrium with the left reservoir, and left movers in equilibrium with the right reservoir. Thus, in the presence of a nonzero source-to-drain voltage, opposite moving edge modes on a given edge will be out of equilibrium with one another.

But since these modes are in close proximity, what stops them from equilibrating? In the effective action (2.7) and (2.8) there are simply no terms that transfer charge between the different edge modes, to allow for possible equilibration. But surely in real experimental systems there will be equilibration processes present. A constraint is that charge transfer between edge modes must conserve momentum along the edge. However, different edge modes will have different momenta—the gauge invariant momentum difference between two modes being proportional to the magnetic flux threading the space between them. Since in equilibrium the different edge modes are at the same energy, processes which transfer charge between two edge modes, with the emission of phonons or photons to take up the momentum, will not conserve overall energy. These processes are thus forbidden.

However, if there are impurities near the edge, as there will be in any real sample, the momentum of the edge modes need not be conserved. Momentum can be transferred to the center of mass of the crystal sample, through the impurities. Thus, a disordered edge with impurity scattering will allow for possible equilibration between the different edge modes. In Sec. III, we study the effect of impurity edge scattering. Before doing so, it is useful to first establish the existence of a special SU(n) symmetry in the action S_0. This symmetry will be crucial in arriving at a solution of the disordered edge.

C. SU(n) symmetry of S_0

It has been known for some time that the structure of the K matrix at filling $\nu = n/(np+1)$ implies that Eq. (2.1) possesses a hidden SU(n) symmetry.[22,27] This is most readily seen for the special case $p = 0$, which corresponds to the integer quantum Hall effect with filling $\nu = n$. However, additional nonuniversal terms should be added to (2.1) (for example, terms with two or more derivatives), and these terms will not respect the SU(n) symmetry. So, in general, the SU(n) symmetry is not expected to be manifest in the bulk. Again, this can be seen clearly in the integer quantum Hall effect ($p = 0$), where the quasihole excitation energies in the n full levels will not be the same.

The SU(n) symmetry implied by the form of the K matrix is also manifest at the edge. For the integer Hall effect ($p = 0$) the SU(n) symmetry is apparent in the edge action S_0, which corresponds to n identical channels of chiral fermions. However, as in the bulk, this symmetry will, in general, be broken by nonuniversal terms, for example, the velocity matrix V_{ij} in S_1, which has no special symmetry properties.

A random edge potential will introduce additional terms, which also break the SU(n) symmetry. However, the very presence of these random terms drives the edge at low energies into a phase in which the SU(n) symmetry is restored. This will also be the case for nonzero p.

We now show that the action S_0 has an SU(n) symmetry even for nonzero p. This will be accomplished via a transformation which decouples the charge degree of freedom, described by $\phi_\rho = \sum_i \phi_i$, from the remaining neutral degrees of freedom. The neutral sector can then be mapped onto the neutral sector of a $\nu = n$ edge, which is described by SU(n) chiral fermions. It is useful to first introduce some SU(n) notation. We denote the $n-1$ diagonal generators as D^m with $m = 1, 2, ..., n-1$. To be specific, we take D^m to be $n \times n$ diagonal matrices with m ones along the diagonal, starting from the upper left, with the next diagonal element being $-m$, to make the matrix traceless. The matrices are then divided by a normalization factor $\sqrt{m^2+m}$ to make $\mathrm{tr}(D^m D^m) = 1$. We denote the $n(n-1)$ nondiagonal generators of SU(n) as R^{ij}, $(i \neq j = 1, 2, ..., n)$, which have a single nonzero matrix element, the (ij) element, equal to one.

The decoupling of the charge and neutral sectors may be performed by defining new fields

$$\Phi_i = O_{ij}\phi_j \ , \tag{2.20}$$

where the matrix O_{ij} is an orthogonal transformation, $O^T O = 1$, given by

$$O_{ij} = D^i_{jj} \tag{2.21}$$

for $i = 1, 2, ..., n-1$ (no sum on j) and

$$O_{nj} = 1/\sqrt{n}. \tag{2.22}$$

It can be readily checked that this transformation diagonalizes the matrix K, giving for $\tilde{K} = OKO^{-1}$ a diagonal matrix of the form $\tilde{K}_{ij} = \delta_{ij}(1+np\delta_{in})$. Upon defining a charge field $\phi_\rho = \sqrt{n}\Phi_n = \sum_i \phi_i$, so that the total edge density is given by $\rho = \partial_x\phi_\rho/2\pi$, the action S_0 is seen to decouple into a charge and neutral sector, $S_0 = S_\rho + S_\sigma$, with

$$S_\rho = \int dxd\tau \frac{1}{4\pi}\left[\frac{1}{\nu} i\partial_\tau\phi_\rho\partial_x\phi_\rho + v(\partial_x\phi_\rho)^2\right] \tag{2.23}$$

and

$$S_\sigma = \int dxd\tau \frac{1}{4\pi}\sum_{i=1}^{n-1} \partial_x\Phi_i(i\partial_\tau + v\partial_x)\Phi_i. \tag{2.24}$$

Notice that when the even integer p is negative, $\nu = n/(np+1)$ is negative, and the charge mode moves in a direction opposite to the $(n-1)$ neutral modes.

In order to make the SU(n) symmetry more explicit, we map S_σ onto the neutral sector of SU(n) fermions. To accomplish this, we introduce an additional auxiliary field, $\tilde{\Phi}_n$, which has an action identical to each of the neutral modes in S_σ. Upon adding this action to it, one has

$$S_\sigma \to \int dxd\tau \frac{1}{4\pi}\sum_{i=1}^{n} \partial_x\tilde{\Phi}_i(i\partial_\tau + v\partial_x)\tilde{\Phi}_i \ , \tag{2.25}$$

where we have defined $\tilde{\Phi}_i = \Phi_i$ for $i = 1, 2, ..., n-1$. It is finally convenient to rotate back, via $\tilde{\phi}_i = O_{ji}\tilde{\Phi}_j$, which leaves the form for S_σ unchanged. The final step is to fermionize the resulting boson fields

$$\psi_i \propto e^{i\tilde{\phi}_i}. \tag{2.26}$$

In this way the free action can finally be expressed as

$$S_0 = S_\rho + \int dxd\tau\psi^\dagger(\partial_\tau - iv\partial_x)\psi \ , \tag{2.27}$$

where ψ here denotes an n-component fermion field. The SU(n) symmetry of the neutral sector is thus manifest. The U(1) charge sector of the above chiral fermions is precisely the auxiliary field $\tilde{\Phi}_n$, introduced above. This field does not enter into any physical quantities, but allows for the above convenient (fermion) representation of the SU(n) symmetry in the neutral sector.

III. THE RANDOM EDGE

Having established the inadequacies of the clean edge, described by the effective action (2.7) and (2.8), we consider now the effects of edge impurity scattering, which allows for interchannel equilibration. With disorder present we will show that the low-temperature physics is described by a new random fixed point, that can be solved exactly.

In the presence of impurity scattering, there are many different types of random edge operators, which can be added to the pure action $S_0 + S_1$ given in (2.7) and (2.8). Here we focus on those that are most relevant. The simplest random terms will take the form

$$\frac{1}{2\pi}\int dxd\tau \sum_i \mu_i(x)\partial_x\phi_i \ , \tag{3.1}$$

where the μ_i are spatially dependent random potentials, which couple to the density in each mode. These terms are unimportant, however, since they can be eliminated from the action via a transformation,

$$\phi_i(x) \to \phi_i(x) + \int_{-\infty}^{x} dx' \sum_j M_{ij}\mu_j(x'), \tag{3.2}$$

where $M_{ij}^{-1} = v\delta_{ij} + V_{ij}$.

More important are random terms that tunnel quasiparticles between the n edge modes, allowing for equilibration. The most relevant operator, which tunnels charge between channel i and j is given by $\exp i(\phi_i - \phi_j)$. A random impurity potential will give rise to terms in the action of the form

$$S_{\text{random}} = \int dxd\tau \sum_{i>j}\left[\xi_{ij}(x)e^{i(\phi_i-\phi_j)} + \text{H.c.}\right] \ , \tag{3.3}$$

where $\xi_{ij}(x)$ are spatially random tunneling amplitudes between edge modes i and j. These amplitudes are complex because the different edge channels have different momenta. Indeed, for a clean edge, the tunneling amplitude would oscillate, as $\exp ik_{ij}x$, where the gauge invariant momentum difference k_{ij} is proportional to the magnetic flux per unit length enclosed between the two channels. This would be ineffective at equilibrating; however, with impurity scattering present, momentum of the edge modes is not conserved, and equilibration can take place.

Since the operators entering into S_{random} are nonlinear in the boson fields, the full random model appears rather intractable. One approach is to study the effects of the random potential $\xi_{ij}(x)$ in perturbation theory about the free theory, $S_0 + S_1$. This is problematic, however, because the perturbation theory is divergent at low energies. One can, nevertheless, define a perturbative renormalization-group transformation in powers of the variance, W_{ij}, defined via $[\xi_{ij}^*(x)\xi_{ij}(0)]_{\text{ens}} = W_{ij}\delta(x)$, where the square brackets denote an ensemble average over realizations of the disorder.[29] The leading order renormalization-group flow equations take the form

$$\frac{\partial W_{ij}}{\partial \ell} = (3 - 2\Delta_{ij})W_{ij} \ , \tag{3.4}$$

where Δ_{ij} is the scaling dimension of the operator $\hat{O}_{ij} = \exp[i(\phi_i - \phi_j)]$ evaluated in the free theory, defined as $\langle O^\dagger(\tau)O(\tau=0)\rangle \sim \tau^{-2\Delta}$. These scaling dimensions are computed explicitly in Appendix A. At the SU(n) symmetric point, where $S_1 = 0$, we find that $\Delta_{ij} = 1$ for all of the tunneling operators. This fact is most easily seen

by exploiting the fermionic representation described in Sec. II. It follows that for $S_1 = 0$ weak disorder is relevant, and grows stronger under scaling to low energies, for all $\nu = n/(np+1)$. Moreover, as discussed in Sec. IV, for non-negative p the scaling dimension does not depend on the nonuniversal velocities which enter into the action S_1. Thus, for all fillings ν with non-negative p, weak disorder is relevant, and must be treated nonperturbatively. For fillings with negative p, such as $\nu = 2/3$, the scaling dimensions Δ_{ij} will vary with the nonuniversal velocities entering in S_1. If these velocities are tuned so that Δ exceeds 3/2, then there will be an edge phase transition into a phase in which disorder is irrelevant. For filling $\nu = 2/3$, this phase transition was analyzed in Ref. 20. In this paper, we will confine our attention to the phase in which $\Delta_{ij} < 3/2$, where the disorder is relevant.

At finite temperatures, some information can be obtained using perturbation theory in the impurity strength. This will be discussed in Sec. III C, and in more detail in Appendix B. However, it is clear that the low-temperature physics lies outside of the perturbative regime. As we now show, however, it is possible to use the fermionic representation of the SU(n) symmetric model (with $S_1 = 0$) to obtain an exact solution for arbitrary disorder strength. In Sec. III B we go on to show that the resulting random fixed point is stable to weak perturbations (nonzero S_1), so that this soluble model provides a description of the low-temperature physics in the entire disorder dominated phase.

A. Exact solution: The random fixed point

Consider then the addition of random edge scattering terms (3.3) to the SU(n) invariant action $S_0 = S_\rho + S_\sigma$ in (2.27). While such terms naively break the SU(n) symmetry, the solution below reveals the presence of a hidden but still exact SU(n) symmetry in this random problem. It is useful to first reexpress $S_{\rm random}$ in (3.3) in terms of the fermion fields appearing in S_0 in (2.27). Under the transformations described in Sec. II C, $\phi_i - \phi_j \to \tilde{\phi}_i - \tilde{\phi}_j$, so we may identify

$$e^{i(\phi_i - \phi_j)} \to \psi^\dagger R^{ij} \psi. \tag{3.5}$$

Here R^{ij} is the off-diagonal SU(n) generator defined in Sec. II. This allows us to rewrite $S_{\rm random}$ in terms of fermion fields as

$$S_{\rm random} = \int dx d\tau \psi^\dagger M(x) \psi \ , \tag{3.6}$$

where $M(x)$ is a random $n \times n$ matrix,

$$M(x) = \sum_{i>j} [\xi_{ij}(x) R^{ij} + \xi^*_{ij}(x) R^{ji}]. \tag{3.7}$$

Notice that the charge sector S_ρ is completely unaffected by the random tunneling. In addition, the neutral sector, $S_\sigma + S_{\rm random}$ is purely bilinear in the Fermi fields, but with a spatially random coefficient, $M(x)$. These random terms act as SU(n) symmetry breaking fields on the quadratic action S_σ. However, they can be eliminated from the action by defining a new set of fermion fields, $\tilde{\psi}$, which are related to the original fermions via a suitable spatially dependent SU(n) rotation. Specifically, upon defining a new fermion field,

$$\tilde{\psi}(x) = U(x)\psi(x) \tag{3.8}$$

with a unitary SU(n) rotation

$$U(x) = T_x \exp\left[\frac{i}{v}\int_{-\infty}^{x} dx' M(x')\right] \tag{3.9}$$

with T_x an x-ordering operator, the action becomes simply

$$S_0 + S_{\rm random} = S_\rho + \int dx d\tau \tilde{\psi}^\dagger (\partial_\tau - iv\partial_x)\tilde{\psi}. \tag{3.10}$$

The action is quadratic in terms of these new rotated fermion fields, with the neutral sector still possessing a full SU(n) symmetry. We have successfully eliminated all random terms by exploiting the SU(n) symmetry present in the pure action S_0. Since the transformed action is quadratic and the disorder does not occur explicitly, we can define a simple renormalization-group (RG) transformation on ϕ_ρ and the rotated fermions, $\tilde{\psi}$, which leaves the action invariant. Our exact solution thus describes a fixed point, with a U(1) charge symmetry and an SU(n) symmetry in the neutral sector. However, it must be borne in mind that we are actually describing a random fixed point, with correlation functions of the original fields depending on the randomness via the above random SU(n) rotation.

B. Stability of random fixed point

Having established that the action $S_0 + S_{\rm random}$ decouples into independent charge and neutral sectors, we must now take into account the nondiagonal interaction matrix in S_1, which we have ignored above. Being nonrandom, these terms couple the charge and neutral sectors and break the SU(n) symmetry even after ensemble averaging over the disorder. However, as we now show, these terms are irrelevant at the random fixed point described by (3.10). The randomness is crucial to guarantee the irrelevance of these operators. As we shall see, without the inclusion of randomness, which is "hidden" in the representation (3.10), the symmetry breaking perturbations in S_1 are not driven to zero.

It is convenient to reexpress S_1 in terms of the fields appearing in (3.10), namely, the charge field ϕ_ρ, and neutral fermion fields $\tilde{\psi}$. Upon performing the orthogonal transformation described in Sec. II C, it is apparent that S_1 in (2.8) can be reexpressed as a sum of three types of terms:

$$S_{1a} = \int dx d\tau v_a (\partial_x \phi_\rho)^2, \tag{3.11}$$

$$S_{1b} = \int dx d\tau \sum_{i,j=1}^{n-1} v_b^{ij} \partial_x \Phi_i \partial_x \Phi_j, \tag{3.12}$$

$$S_{1c} = \int dx d\tau \sum_{i=1}^{n-1} v_c^i \partial_x \phi_\rho \partial_x \Phi_i. \tag{3.13}$$

The coefficients v_μ (with $\mu = a, b, c$) can be expressed in terms of the velocity matrix V_{ij}. The first term, involving v_a, is innocuous and can be absorbed into S_ρ, giving a shift in the velocity of the charge mode. To analyze the other terms, it is useful to reexpress the boson fields Φ in terms of the fermion fields

$$\frac{1}{2\pi}\partial_x \Phi_m \to \psi^\dagger D^m \psi \to \tilde{\psi}^\dagger M^m(x) \tilde{\psi} \ , \tag{3.14}$$

where $M^m(x)$ are $n \times n$ matrices given by

$$M^m(x) = U(x) D^m U^\dagger(x) \ , \tag{3.15}$$

with $U(x)$ defined in (3.9). The unitary matrix $U(x)$ is a random x-dependent SU(n) rotation, which is uncorrelated on scales long compared to a mean free path for interchannel scattering, $\ell \sim v_\sigma^2/W$. Thus, $M^m(x)$ will similarly be random $n \times n$ matrices. Treating v_b as small, we can now show that the SU(n) fixed point described by (3.10) is stable to this perturbation. Note first that the operator in S_{1b} involves four fermion fields, $\tilde{\psi}$, and so has a scaling dimension of $\delta = 2$, at the SU(n) fixed point described by (3.10). Since the coefficient of this operator is spatially random, we consider the linear RG flow equation for its mean square average, $W_b \propto v_b^2$, which is of the form,

$$\frac{\partial W_b}{\partial \ell} = (3 - 2\delta) W_b. \tag{3.16}$$

The perturbation is clearly irrelevant. It should be emphasized that in the absence of randomness, the dimension 2 operators in S_{1b} are marginal and do not renormalize to zero. Thus, disorder is seen to be absolutely critical in the stability of the SU(n) fixed point (3.10). The reason why the random perturbation is irrelevant, while the uniform perturbation is marginal, can be understood as follows. The mean square average of the random perturbation over a length scale $L \gg \ell$, is an average over L/ℓ uncorrelated regions, and will hence decay as L^{-1}. This accounts for the renormalization-group eigenvalue of -1 in (3.16).

The above argument can also be used for the perturbation S_{1c} in (3.13), which mixes the charge and neutral sectors. This operator also has a scaling dimension of $\delta = 2$, and will have a spatially random coefficient $v_c(x)$. The variance W_c of $v_c(x)$ obeys a linear RG flow equation identical to (3.16) and will likewise scale to zero under a RG transformation.

We thus see that the disorder has played a crucial role in both driving the charge/neutral coupling to zero, and driving the SU(n) symmetry breaking interactions in the neutral sector to zero. The final fixed point theory, described by (3.10), has a full U(1)×SU(n) symmetry, a much higher symmetry than the underlying random Hamiltonian.

C. Finite temperatures: The hydrodynamic regime

The exact solution (3.10) of the random edge that describes a stable zero-temperature fixed point can also be used to extract physical properties of the edge at low but nonzero temperatures. These properties will be determined by the structure of the fixed point itself, and the leading irrelevant operators, such as those proportional to v_μ above. At low but nonzero temperatures, these operators have not had "time" to fully renormalize to zero, and can then have an important effect on physical observables. Although one can show that the irrelevant operators do not modify the quantized Hall conductance itself, they do dramatically effect the propagation of the neutral modes at finite temperature.

To see why, we first note that the existence of the propagating neutral modes is tied intimately to the exact SU(n) symmetry in the neutral sector at the fixed point. But at finite temperatures, this symmetry is no longer exact, due to the presence of irrelevant operators, so that the neutral modes should no longer be strictly conserved. Thus, one expects that at finite temperatures the neutral modes should decay away at a nonvanishing rate, $1/\tau_\sigma$. Equivalently, one expects a finite decay length, or "inelastic scattering length," $\ell_\sigma = v_\sigma \tau_\sigma$. On scales L much larger than ℓ_σ, the neutral modes should not propagate. Since the fixed point is approached as $T \to 0$, however, the decay length should diverge in this limit.

At wavelengths long compared to ℓ_σ, we thus expect a hydrodynamic regime, in which the only propagating modes are those required by conservation laws. Since the only conserved quantity in this regime is the total electric charge, we expect a single propagating "zero sound" mode.

In order to establish the existence of the hydrodynamic regime and to compute the temperature dependence of the neutral mode decay rate, we evaluate the self-energy of the neutral mode perturbatively about the random fixed point (3.10). The dominant contributions come from the interactions v_b and v_c in Eqs. (3.12) and (3.13). Notice that (3.13) contains terms of the form

$$\delta S = \int dx d\tau \tilde{v}_c^{ij}(x) \partial_x \phi_\rho \tilde{\psi}^\dagger R^{ij} \tilde{\psi} + \text{c.c.} \ , \tag{3.17}$$

where $\tilde{v}_c^{ij}(x)$ is a random coefficient which depends, as in (3.15), on the random SU(n) rotation. Breaking the SU(n) symmetry, this term explicitly violates the conservation of the neutral modes.

It is convenient at this stage to rebosonize the "rotated" fermion fields. We thus "undo" the steps that lead us from Eqs. (2.24) to (2.27), writing $\tilde{\psi}_i = \exp(i\tilde{\chi}_i)$, and $\tilde{\chi}_i = O_{ji}\chi_j$. [In the absence of disorder we would thus have $\chi_i = \Phi_i$ in (2.24).] In terms of these new bosonic fields, the fixed point action in (3.10) now takes the form

$$S_0 + S_{\text{random}} = S_\rho + \int dx d\tau \frac{1}{4\pi} \sum_{i=1}^{n-1} \partial_x \chi_i (i\partial_\tau + v\partial_x)\chi_i, \tag{3.18}$$

where we have omitted the auxiliary "charge" mode, χ_n.

In this representation, we can now evaluate the self-energy for χ_i perturbatively in $\tilde{v}$. For simplicity, we consider here only contributions from the term $\tilde{v}^{12}$ in (3.17) for which the corresponding operator has a particularly nice bosonized representation,

$$\partial_x \phi_\rho \tilde{\psi}^\dagger R^{12} \tilde{\psi} = \partial_x \phi_\rho e^{i\sqrt{2}\chi_1}, \tag{3.19}$$

where

$$\partial_x \chi_1 = \frac{1}{\sqrt{2}} \partial_x (\tilde{\chi}_1 - \tilde{\chi}_2) = \tilde{\psi}^\dagger D^1 \tilde{\psi}. \tag{3.20}$$

Since the perturbation v_{12} only involves χ_1, its effects will be contained in the retarded Greens function

$$G_1^R(x,t) = \langle [\chi_1(x,t), \chi_1(0,0)] \rangle \theta(t). \tag{3.21}$$

When evaluated at the fixed point (3.18) it takes the simple form

$$G_1^{0R}(q,\omega) = \frac{2\pi}{q(\omega + i\epsilon - vq)}, \tag{3.22}$$

exhibiting a pole at the neutral mode frequency, $\omega = vq$.

For simplicity, we take the random coefficient $\tilde{v}^{12}$ to be δ correlated in space, with variance W_c. The self-energy may then be evaluated perturbatively in W_c. To lowest order, the self-energy involves the diagrams shown in Fig. 3. These are evaluated in Appendix B, where we show that at low frequencies,

$$\Sigma(q,\omega) = \frac{i\omega}{2\pi \ell_\sigma}, \tag{3.23}$$

with $\ell_\sigma^{-1} \propto W_c T^2$. Unfortunately, this lowest order approximation to the self-energy leads to an incorrect description of the long wavelength limit, inconsistent with the hydrodynamic regime. In Appendix B we show that the correct self-energy, obtained by summing a class of diagrams, is given by

$$\Sigma(q,\omega) = \frac{i\omega}{2\pi \ell_\sigma} \frac{1}{1 - i(q\ell_\sigma)^{-1}}. \tag{3.24}$$

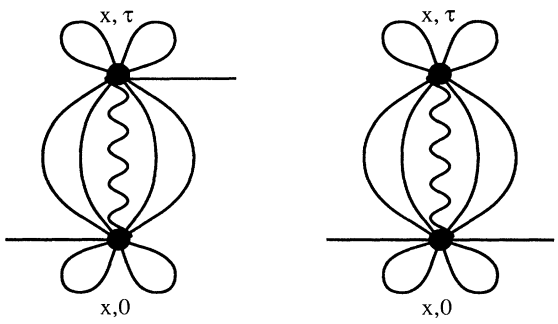

FIG. 3. Diagrams for the self-energy of the Greens function in (3.21). The solid circles represent the interaction (3.19). The solid lines represents the bare propagator for χ_1, G_1^0, and a sum over all possible combinations of these lines is implied. The wavy line represents the bare propagator for ϕ_ρ.

Note that to leading order in W_c (or ℓ_σ^{-1}) (3.24) reduces to (3.23). However, higher order terms in the expansion are singular in the $q \to 0$ limit and must be accounted for in the correct long wavelength theory.

Using (3.24), we may then write the retarded neutral boson Green's function as

$$G_1^R(q,\omega) = 2\pi \frac{1 - i(q\ell)^{-1}}{q(\omega - v_\sigma q + i/\tau_\sigma)}, \tag{3.25}$$

which exhibits a neutral mode decaying at a rate

$$\frac{1}{\tau_\sigma} = v_\sigma / \ell_\sigma \propto W_c T^2. \tag{3.26}$$

An analogous calculation leads to a similar result for the interactions given by v_b in Eq. (3.12). At nonzero temperatures, the neutral mode decays away, just as for a quasiparticle in a Fermi liquid.

The effects of the irrelevant operators on the charge mode may be evaluated in a similar manner. However, due to charge conservation we do not expect the charge mode to decay. Indeed, it can be seen explicitly that the interaction terms in (3.11)–(3.13) commute with the total charge. Consider the Greens function for the charge mode

$$G_\rho^R(x,t) = \langle [\phi_\rho(x,t), \phi_\rho(0,0)] \rangle \theta(t), \tag{3.27}$$

which at the fixed point (3.10) is given by

$$G_\rho(q,\omega) = \frac{2\pi}{q(\omega + i\epsilon - v_\rho q)}. \tag{3.28}$$

The contribution to the self-energy due to the interaction (3.13) may be computed along the same lines as above, and we find

$$\Sigma_\rho(q,\omega_n) \propto i\omega q^2 W_c \,. \tag{3.29}$$

This leads to a correction to the charge mode propagator, which becomes

$$G_\rho(q,\omega) = \frac{2\pi}{q(\omega - v_\rho q + iDq^2)}. \tag{3.30}$$

This form implies that a localized charge pulse will spread diffusively as it propagates down the edge with a temperature-independent diffusion constant $D \propto W_c$. As expected, though, due to charge conservation the decay rate vanishes at $q = 0$, in contrast to the neutral modes.

By working perturbatively about the random fixed point (3.10), we have thus shown that at finite temperatures, on length scales long compared to $\ell_\sigma \propto T^{-2}$, there exists a hydrodynamic regime characterized by a single propagating charge mode. It is also instructive to recover this hydrodynamic regime by working perturbatively about the fixed line in the absence of randomness, described by (2.7) and (2.8). This will be valid at high temperatures when weak disorder has not had "time" to flow out of the perturbative regime. Like the random fixed point, the clean fixed line also has higher symmetry because each of the n propagating modes are inde-

pendently conserved. As explained in Sec. II B, this implies a conductance which is not quantized when channels move in opposite directions. However, even weak interchannel scattering destroys the independent conservation laws, leaving total charge as the only conserved quantity. We thus expect a long wavelength hydrodynamic regime with only a single propagating charge mode. In Appendix B, we analyze the effects of randomness perturbatively and establish this hydrodynamic regime on length scales longer than the mean free path ℓ for interchannel scattering, given by

$$\ell^{-1} \propto W T^{2\Delta-2} , \tag{3.31}$$

where W is the rms strength of the randomness and Δ is the scaling dimension of the tunneling operator. Moreover, we find that in this hydrodynamic regime the quantization of the conductance is restored, giving $G = \nu e^2/h$ even when $p < 0$.

IV. TUNNELING AT THE EDGE

We now apply the theory described above to compute the scaling dimension of general edge tunneling operators. These scaling dimensions determine the temperature exponents for tunneling through a point contact[11,26] between two Hall fluids.

The most general edge tunneling operator can be written

$$\hat{T}(x) = e^{i \sum_{j=1}^{n} m_j \phi_j(x)} \tag{4.1}$$

for arbitrary integers m_j. This operator creates an edge quasiparticle excitation at position x, with charge Q given by

$$Q = \sum_{ij} m_i K^{-1}_{ij}. \tag{4.2}$$

This is the same value as the bulk quasiparticle charge (2.5). For filling factor $\nu = n/(np+1)$, the inverse of the K matrix is, $K^{-1}_{ij} = \delta_{ij} - p/(np+1)$, which gives for the charge

$$Q = \nu \bar{m}, \tag{4.3}$$

with the definition

$$\bar{m} = \frac{1}{n} \sum_{j=1}^{n} m_j. \tag{4.4}$$

For non-negative p, the charge and neutral modes propagate in the same direction. In this case, we prove in Appendix A that even in the absence of randomness, the scaling dimension of the tunneling operator is independent of the (nonuniversal) velocity matrix in S_1 (2.8). This can be understood by considering the form of the correlation function computed in the absence of randomness,

$$P(x,\tau) = \langle \hat{T}(x,\tau)^\dagger \hat{T}(0,0) \rangle \propto \prod_{i=1}^{n} \frac{1}{(v_i \tau + i x)^{\delta_i}}, \tag{4.5}$$

where the expectation value is taken with respect to the action $S_0 + S_1$ in (2.7) and (2.8). Each eigenmode of the quadratic action contributes one term to the product in (4.5). The scaling dimension of $\hat{T}$ is then given by $2\Delta = \sum_i \delta_i$. There is a constraint on the δ_i, though, due to the statistics of the quasiparticle. The operator $\hat{T}$ creates an edge quasiparticle that must have the same statistics as a bulk quasiparticle. The statistics of the edge quasiparticle can be defined as the phase accumulated upon rotating x, τ to $-x, -\tau$ clockwise in the Euclidean plane, since for $\tau = 0$ this effectively interchanges two quasiparticles. In Appendix A, we verify by explicit calculation that the "edge" statistics angle defined in this way indeed equals the bulk statistics angle given in (2.6). Since for $p \geq 0$ all of the velocities v_i have the same sign, under this exchange $P \to P \exp i\Theta$, with a statistics angle $\Theta/\pi = \sum_i \delta_i$. Generally, the statistics angle is a topological property of the bulk quantum Hall state, is universal and independent of the edge interaction matrix V_{ij}. But for non-negative p, the scaling dimension of the edge tunneling operator equals the statistics angle, $2\Delta = \Theta/\pi$ and is, therefore, also universal.

To describe tunneling at a point contact, the relevant quantity is the local scaling dimension of the edge tunneling operator, defined via $P(x = 0, \tau) \sim \tau^{-2\Delta}$. This average is independent of the spatially random SU(n) rotation of Sec. III. Thus, for $p \geq 0$, the local scaling dimension is still given by the (bulk) quasiparticle statistics, even in the presence of disorder. We thus have from (2.6),

$$2\Delta = \sum_{ij} m_i K^{-1}_{ij} m_j. \tag{4.6}$$

For bulk filling $\nu = n/(np+1)$, this can be written as

$$2\Delta = \frac{Q^2}{\nu} + \sum_{j=1}^{n} (m_j^2 - \bar{m}^2). \tag{4.7}$$

When p is negative, the charge mode propagates in the direction opposite to the neutral modes, so that the velocities in (4.5) are no longer all of the same sign. The constraint imposed by the bulk quasiparticle statistics, therefore, becomes $\Theta/\pi = \sum_i \mathrm{sgn}(v_i)\delta_i$, and no longer determines the scaling dimension of the edge tunneling operator, $2\Delta = \sum_i \delta_i$. Thus, in the absence of random tunneling terms, $S_{\mathrm{random}} = 0$, the scaling dimension of $\hat{T}$ is nonuniversal depending on the velocity matrix V_{ij} in S_1. However, with randomness present, the system flows to the fixed point (3.10), which has an exact U(1)×SU(n) symmetry. The local scaling dimension of the edge tunneling operators $\hat{T}$ then follow from the universal properties of this fixed point.

To evaluate them it is useful to reexpress the tunneling operator in terms of the charge and neutral fields. We find

$$\hat{T} = e^{i\bar{m}\phi_\rho} \prod_{i=1}^{n} \psi_i^{(m_i - \bar{m})}. \tag{4.8}$$

Being interested only in the local scaling dimension, we

can replace ψ by $\tilde{\psi}$ in the above. Then upon evaluating the average in (4.5) using the quadratic fixed point action (3.10) gives

$$2\Delta = \frac{Q^2}{|\nu|} + \sum_{j=1}^{n}(m_j^2 - \bar{m}^2) \ . \tag{4.9}$$

The first term comes from the charge mode, and the second contribution from the neutral sector. Notice that this form is the same as that for $p \geq 0$, except with a modulus of ν.

We note here that the irrelevant operators discussed in Sec. III C, which lead to a finite lifetime for the neutral mode at finite temperatures, do not affect our results for the tunneling exponents. The finite lifetime introduces a $1/\tau_\sigma \propto T^2$ cutoff into the logarithmically divergent integral, which occurs in the exponent when the correlation function $\langle \hat{T}(\tau)\hat{T}(0)\rangle$ is computed. But this divergence is already cut off by the temperature T so at low temperatures the finite lifetime has no effect. Thus, even though the neutral mode is not conserved at finite temperature, it has a crucial effect on the asymptotic temperature dependence of the tunneling exponents.

With our final expressions for the local scaling dimensions of the most general edge tunneling operators, we are in position to make quantitative predictions for a number of interesting experiments.

V. EXPERIMENTAL IMPLICATIONS

The simplest experiment that is sensitive to the edge dynamics involves making a constriction or point contact in a quantum Hall fluid. At the constriction, the top and bottom edges of the Hall bar are close together, as shown in Fig. 4, facilitating tunneling processes between the two edges. Any charge that tunnels between the edges is effectively backscattered, and will reduce the source to drain conductance. The local scaling dimension of the edge tunneling operators will then feed into the temperature dependence of the conductance through the constriction.

Consider first the limit of a very slight constriction, which will give a small amount of backscattering. In this regime, the temperature dependence of the conductance through the constriction will be dominated by the quasiparticle, which can tunnel most easily from top to bottom edge. The amplitude for such tunneling, though, will in general be temperature dependent, and at low temperatures will be dominated by the quasiparticle with the smallest scaling dimension. To leading order the conductance will take the form[26]

$$G(T) = |\nu|\frac{e^2}{h} - v^2 T^{2(2\Delta_{\min}-1)} + O(v^4), \tag{5.1}$$

where v is the amplitude for the tunneling of this quasiparticle.

A charge $Q = \nu$ quasiparticle with scaling dimension $2\Delta = |\nu|$ can be obtained from (4.1) by taking $m_j = 1$ for all j. On the other hand, a single $m_j = 1$ with the rest equal to zero creates an n-fold degenerate excitation with charge ν/n and scaling dimension $2\Delta = 1 - 1/n - |\nu|/n^2$. For the integer quantum Hall effect, $\nu = n$ ($p = 0$), the latter corresponds to a quasiparticle with the smallest dimension, $2\Delta_{\min} = 1$. Physically, it corresponds to tunneling an electron into one of the n edge channels. As expected, the backscattering which reduces the conductance in (5.1), is independent of temperature in this case.

For all fractional quantum Hall states ($p \neq 0$) *except* $\nu = 2/3$ ($n = 2, p = -2$), the charge ν quasiparticle has the smallest dimension, so that

$$2\Delta_{\min} = |\nu|. \tag{5.2}$$

Notice that with $|\nu| < 1$ the backscattering corrections grow at low temperatures. The above form (5.1) is only valid down to temperatures where the corrections to the quantized conductance remain small.

By varying parameters, such as a gate voltage, it should be possible to tune the amplitude of the leading relevant backscattering to zero. This will appear as a resonance in the conductance. The robustness of the resonances at low temperatures, that is the temperature dependence of the resonance peak, will be determined by the backscattering of the quasiparticle with the next smallest scaling dimension. If this scaling dimension is larger than 1/2, then the conductance on resonance will be perfect, and the resonance robust. In this case, one expects that the resonance line shape should be universal, as predicted for $\nu = 1/3$. If less than 1/2, the resonance peak will diminish in amplitude upon cooling and eventually vanish completely in the zero-temperature limit. In either case, there should be a regime in temperature where the width of the resonance narrows upon cooling, varying as $T^{(1-|\nu|)}$.

For the special case $\nu = 2/3$ it turns out that the quasiparticle tunneling operators with $(m_1, m_2) = (1,0)$, $(0,1)$, and $(1,1)$ all have the same dimension. The dimension is still given by (5.2), but now the most relevant operator is not unique, but threefold degenerate. This suggests that resonances for $\nu = 2/3$ will tend to be less robust than for the other fractions.

Away from resonances, in the fractional Hall effect ($p \neq 0$), the conductance through the constriction drops with decreasing temperature, eventually invalidating the

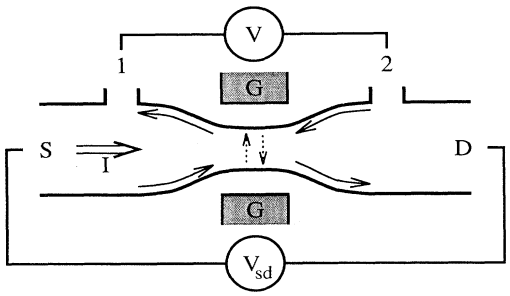

FIG. 4. Schematic portrait of a point contact, in which the top and bottom edges are brought together by an electrostatically controlled gate, allowing for the tunneling of charge between the two edges.

perturbative result (5.1). In this regime, we can consider the opposite limit of large backscattering, where the dominant process is physical electrons tunneling through the point contact from one side to the other. In this limit, the conductance will be dominated by the charge $Q = 1$ tunneling operator, which has the smallest scaling dimension, varying with temperature as[26]

$$G(T) \approx t^2 T^{2[2\Delta_{\min}(Q=1)-1]}. \tag{5.3}$$

Here t is the amplitude for the dominant electron tunneling process. The scaling dimension $\Delta_{\min}$ for $Q = 1$ can be obtained by taking $m_j = p + \delta_{jk}$ for $k = 1, ..., n$, in (4.1), which gives

$$2\Delta_{\min}(Q = 1) = \frac{1}{|\nu|} + 1 - \frac{1}{n}. \tag{5.4}$$

This tunneling operator is not unique, but n-fold degenerate.

For non-negative p, when all the edge channels are moving in the same direction, the above two expressions can be combined to give

$$G(T) \approx t^2 T^{2p}. \tag{5.5}$$

For the integer quantum Hall effect, this gives the expected temperature-independent result. For the dominant $p = 2$ sequence, $\nu = 1/3, 2/5, 3/7, 4/9, ...$, this predicts a T^4 temperature dependence.

When p is negative, and the neutral modes are moving in a direction opposite to the charge modes, the conductance can be expressed using (5.3) and (5.4) as

$$G(T) \approx t^2 T^{2|p|-(4/n)}. \tag{5.6}$$

For the $p = -2$ sequence, $\nu = 2/3, 3/5, 4/7, 5/9, ...$, the predicted power laws are $2, 8/3, 3, 31/5, ...$, which approach a T^4 as ν approaches $1/2$. It is worth emphasizing that in this case the particular powers are determined by the structure of the disorder dominated fixed point, at which the neutral and charge sectors decouple. Even though it is electron tunneling that dominates in this regime, the neutral modes are essential. Since an electron is built from a superposition of the charge mode and neutral modes, upon tunneling through the point contact into the edge, the electron excites both the charge and neutral modes.

Another central feature of the random U(1)×SU(n) fixed point is that the $n - 1$ neutral modes are all predicted to move at the same velocity. So, for example, at the edge of an integer quantum Hall state with filling $\nu = 3$, the three edge modes, which will in general have different velocities in the absence of edge randomness, are predicted to decouple with randomness into a charge mode, moving at one velocity, and two neutral modes moving at the same velocity as one another. This decoupling will take place on length scales longer than an edge mean free path. The mean free path depends on the strength of the edge impurity scattering and the spatial separation between the various edge modes, and will thus clearly be a sample specific length. For $\nu = 2$, one has a rather nice example of "spin-charge" separation, with the edge channel index playing the role of the electron spin s_z. The disorder decouples the charge mode from the SU(2) invariant neutral mode, the analog of the "spin mode," and the two modes separate, moving at different velocities.

The edge neutral modes might be directly measurable via suitable low-temperature time domain transport experiments, similar to Ashoori *et al.*[28] In Ashoori *et al.*, the edge states of a quantum Hall sample were excited by sending a short pulse into a capacitor placed near the edge. Another capacitor was used to detect the propagating edge modes, on the other side of the sample. For filling $\nu = 2/3$, only one propagating mode was observed. Our theory predicts the existence of only one charge mode, the other being neutral and presumably coupling very weakly to the capacitors. This could explain naturally the observed absence of a second propagating mode. A suitable generalization of Ashoori *et al.*, which would allow for detection of the neutral modes, would be to replace the capacitors with tunnel junctions. Sending a short pulse of electrons into the edge of a quantum Hall sample, would excite both the charge and neutral modes at the edge. Provided the temperature was low enough that the decay length l_σ exceeds the sample dimensions, the neutral modes could be detected at the far side of the sample with another tunnel junction. The neutral modes, upon passing by the second tunnel junction, would excite electrons to tunnel into the leads, and should be detectable as a time domain current pulse. By varying the temperature, it might also be possible to extract the temperature dependence of the neutral mode decay rate, to test the predicted T^2 dependence. This would be the analog of a direct real-time measurement of a decaying Fermi-liquid quasiparticle.

In this article, we have established the existence of a random edge fixed point for states at filling $\nu = n/(np + 1)$ [with U(1)×SU(n) symmetry], and demonstrated that it is locally stable. It should be emphasized, however, that we have not argued for the absence of other edge phases, at the same bulk filling. It is conceivable that for a given filling ν, there exist other edge phases, separated from the phase we have analyzed by an edge phase transition. In fact, for the special case of $\nu = 2/3$ we know this to be the case. In our earlier paper with Polchinski we found another (locally) stable edge fixed point for $\nu = 2/3$, at which weak random edge tunneling was irrelevant and the charge and neutral sectors did not decouple. In this phase, the two-terminal conductance at $T = 0$ is nonuniversal. However, at finite temperatures the quantization of the conductance is restored, provided the sample is larger than the mean free path for interchannel tunneling (which diverges as $T \to 0$). Moreover, in this disorder-free phase the tunneling exponents were predicted to be nonuniversal. There was a Kosterlitz-Thouless-like zero-temperature phase transition separating the two phases. However, for filling ν with non-negative p, the disorder-free edge phase is always perturbatively unstable to disorder. Thus, if other edge phases exist for these fillings, they will presumably also be described by random fixed points. Ultimately

though, the actual phase for the edge of a given real sample will have to be determined by comparing with the predicted behavior.

It is also worth pointing out that the special SU(n) symmetry at the edge has only been established for the class of Hall states at filling $\nu = n/(np+1)$, with n integer and p an even integer. For other filling fractions not of this form, such as $\nu = 4/5$, there may not be such high symmetry at the edge. The low-energy edge structure at these fillings will be the subject of future work.

In brief summary, we have shown that disorder at the edge of a quantum Hall fluid plays an essential role in determining the structure of the low-energy edge excitations. In particular, for fractional quantum Hall states at filling $\nu = n/(np+1)$, we have shown that the disordered edge actually has a higher symmetry than a perfectly clean edge would have. The charge is carried in a single mode, and the remaining $n-1$ neutral modes all propagate at the same speed and possess an SU(n) symmetry. An exact solution for the random SU(n) fixed point has been presented, which allows for numerous quantitative experimental predictions.

ACKNOWLEDGMENTS

This paper is an extension and generalization of an earlier paper with J. Polchinski (Ref. 20). We are extremely grateful and indebted to him for many of the key ideas and results contained herein. We are also grateful to N. Read, R. Webb, and A. Zee for fruitful discussions. M.P.A.F. has been supported by the National Science Foundation under Grant Nos. PHY89-04035 and DMR-9400142.

APPENDIX A: GENERAL TREATMENT OF MULTICHANNEL CLEAN EDGE

In this appendix, we consider a clean multichannel edge described by the general action

$$S = \int dx d\tau \frac{1}{4\pi} \sum_{ij} \partial_x \phi_i \left[K_{ij}\ i\partial_\tau + v_{ij}\partial_x \right] \phi_j . \quad \text{(A1)}$$

We wish to compute the conductance as well as the scaling dimension and statistics angle of tunneling operators. We show that these quantities are universal if all of the channels propagate in the same direction. In general, however, the conductance and scaling dimensions are nonuniversal. The following analysis is valid for an arbitrary K matrix, and is not limited to quantum Hall edge states at filling factors $\nu = n/(np+1)$.

In order to proceed, it is convenient to transform the problem into a representation in which both K_{ij} and v_{ij} are diagonal. This can be accomplished in three steps. First, we diagonalize the matrix K via an orthogonal transformation $\phi_i = \Lambda_{1,ij}\tilde{\phi}_{1,j}$, where $(\Lambda_1^T \Lambda_1)_{ij} = \delta_{ij}$ and $(\Lambda_1^T K \Lambda_1)_{ij} = \lambda_i \delta_{ij}$. For $\nu = n/(np+1)$, this transformation was performed explicitly in Sec. II: $\Lambda_{1ij} = O_{ij}$ defined in (2.21) and (2.22), and $\lambda_i = 1 + np\delta_{in}$. We then rescale $\tilde{\phi}_{1,i}$ by writing $\tilde{\phi}_{1,i} = \Lambda_{2,ij}\tilde{\phi}_{2,j}$, where $\Lambda_{2,ij} = \delta_{ij}/\sqrt{|\lambda_i|}$. In this representation, the action is

$$S = \int dx d\tau \frac{1}{4\pi} \sum_{ij} \partial_x \tilde{\phi}_{2i} \left(\eta_{ij}\ i\partial_\tau + \tilde{v}_{ij}\partial_x \right) \tilde{\phi}_{2j} , \quad \text{(A2)}$$

with $\tilde{v} = \Lambda_2^T \Lambda_1^T (v_{ij}) \Lambda_1 \Lambda_2$, and $\eta_{ij} = \mathrm{sgn}(\lambda_i)\delta_{ij}$. It is now possible to diagonalize $\tilde{v}$ via a transformation, which preserves the form of η_{ij}. Thus, we let $\tilde{\phi}_{2,i} = \Lambda_{3,ij}\tilde{\phi}_{3,j}$ where, $(\Lambda_3^T \tilde{v} \Lambda_3)_{ij} = \tilde{v}_i \delta_{ij}$ and $\Lambda_3^T \eta \Lambda_3 = \eta$. Λ_3 will have the form of a Lorentz transformation in which $\mathrm{sgn}(\lambda_i) = +1$ and -1 correspond to spacelike and timelike dimensions. We have thereby decoupled the channels, so that

$$S = \int dx d\tau \frac{1}{4\pi} \sum_{i} \partial_x \tilde{\phi}_{3i} \left(\eta_i\ i\partial_\tau + \tilde{v}_i \partial_x \right) \tilde{\phi}_{3i} . \quad \text{(A3)}$$

This gives an explicit description of the eigenmodes of the system. Since stability of the action requires that $\tilde{v}_i > 0$, the direction of propagation of each mode is determined by η_i $(= \eta_{ii})$.

It is now straightforward, using the technique outlined in Sec. II B, to formally compute the edge current

$$I = \sum_{ij} (\Lambda_1 \Lambda_2 \Lambda_3)_{ij} \dot{\tilde{\phi}}_{3j}/2\pi, \quad \text{(A4)}$$

in response to the applied potential $V(x)$, which couples to the total charge density

$$\rho(x) = \sum_{ij} (\Lambda_1 \Lambda_2 \Lambda_3)_{ij} \partial_x \tilde{\phi}_{3j}/2\pi. \quad \text{(A5)}$$

If different channels move in opposite directions, then the current will depend on the voltages in both the left and right reservoirs, V_L and V_R. We find

$$I_{\mathrm{edge}} = \frac{e^2}{h} \sum_{ij} (M_{ij}^+ V_L - M_{ij}^- V_R) , \quad \text{(A6)}$$

where

$$M^\pm = \Lambda_1 \Lambda_2 \Lambda_3 \frac{1 \pm \eta}{2} \Lambda_3^T \Lambda_2^T \Lambda_1^T . \quad \text{(A7)}$$

We may thus write

$$I_{\mathrm{edge}} = \frac{e^2}{h} \left(g_+ V_L - g_- V_R \right) , \quad \text{(A8)}$$

with $g_\pm$ being dimensionless right/left conductances:

$$g_\pm = \sum_{ij} M_{ij}^\pm . \quad \text{(A9)}$$

Noting that $\Lambda_3 \eta \Lambda_3^T = \eta$, it is straightforward to show that

$$M^+ - M^- = K^{-1}, \quad \text{(A10)}$$

which is universal and independent of the velocities v_{ij}.

It then follows from Eqs. (A9) and (2.3) that

$$g_+ - g_- = \nu. \tag{A11}$$

When all of the channels move in the same direction, say $\eta = 1$, then M_- is equal to zero. In this case, $M^+ + M^-$ (and hence $g_+ + g_-$) is also universal. However, when there are channels moving in opposite directions, no such simple relation exists for $M^+ + M^-$. For $\nu = n/(np+1)$, it is possible to use the explicit form of Λ_1 and Λ_2 to write

$$g_+ + g_- = \nu(\Lambda_3 \Lambda_3^T)_{nn}. \tag{A12}$$

In general, Λ_3 will depend on the nonuniversal parameters v_{ij}. It should be noted, however, that when v_{ij} is diagonal, as is the case at the SU(n) symmetric fixed point, then $\tilde{v}_{ij}$ is also diagonal, so that $\Lambda_3 = 1$. In this case $g_+ + g_- = \nu$ even when there are channels moving in opposite directions.

The scaling dimension of a general tunneling operator

$$\hat{T} = e^{i \sum_i m_i \phi_i} \tag{A13}$$

may be deduced from the correlation function

$$P(x,\tau) = \langle \hat{T}(x,\tau) \hat{T}(0,0) \rangle \ . \tag{A14}$$

Using the transformations defined above, this may be simply computed and at zero temperature has the form

$$P(x,\tau) \propto \prod_k \frac{1}{(\eta_k \tilde{v}_k \tau + ix)^{\delta_k}} \ , \tag{A15}$$

where the exponent

$$\delta_k = \sum_{ij} m_i (\Lambda_1 \Lambda_2 \Lambda_3)_{ik} (\Lambda_3^T \Lambda_2^T \Lambda_1^T)_{kj} m_j \ . \tag{A16}$$

The scaling dimension is then determined by

$$2\Delta = \sum_k \delta_k = \sum_{ij} m_i (M_{ij}^+ + M_{ij}^-) m_j. \tag{A17}$$

The "edge" statistics angle, as discussed in Sec. IV, is given by

$$\frac{\Theta_{\text{edge}}}{\pi} = \sum_k \eta_k \delta_k = \sum_{ij} m_i K_{ij}^{-1} m_j, \tag{A18}$$

where we have used (A10). Thus, we see that Θ_{edge}/π is universal and is equal to the bulk quasiparticle statistics angle (2.6). However, the scaling dimension 2Δ is only universal when all of the channels move in the same direction. Otherwise, it is nonuniversal and depends on v_{ij}.

The neutral tunneling operators, which correspond to the tunneling of charge between channels on a given edge, are a special case of the general tunneling operator described above. For $\nu = n/(np+1)$, an arbitrary neutral operator may be written as

$$\hat{T}_{Q=0} = \exp i \sum_{i=1}^{n-1} n_i \Phi_i, \tag{A19}$$

where Φ_i is defined in (2.20). The scaling dimension of this operator may then be shown to be

$$2\Delta_{ij} = \sum_{ij=1}^{n-1} n_i (\Lambda_3 \Lambda_3^T)_{ij} n_j \ . \tag{A20}$$

APPENDIX B: EDGE DYNAMICS AT FINITE TEMPERATURES

In this appendix we analyze the long length scale edge-state dynamics at finite temperatures. Such an analysis arises in two different contexts. In Sec. III, we described the disorder dominated $T = 0$ fixed point which has an SU(n) symmetry, and hence $n-1$ propagating neutral modes in addition to the charge mode. In this case, the leading irrelevant operator which couples the neutral and charged sectors, destroys the SU(n) symmetry and hence violates the conservation of the neutral modes. Thus, at finite temperature, when such operators have not flowed to zero, we expect that the $n-1$ neutral modes will not propagate on long length scales. In this hydrodynamic regime, there should be only a single propagating mode associated with the conserved electric charge.

An analogous situation arises in perturbation theory in the impurity scattering strength about the clean fixed point, described by $S_0 + S_1$ in (2.7) and (2.8). In this case, however, the perturbation theory is generally divergent at zero temperature. Nonetheless, at finite temperatures, perturbation theory can provide some useful information. Like the random fixed point, the clean fixed point has a high symmetry, since the charges in each of the n channels are independently conserved, leading to n propagating modes. As shown in Appendix A, this implies a nonuniversal conductance when any of the channels move in opposite directions. At finite temperatures, however, the interchannel impurity scattering will destroy the independence of the different channels. We, thus, again expect a long wavelength hydrodynamic regime in which only a single propagating charge mode should exist. Moreover, as we shall show below, in this hydrodynamic regime, the conductance is universal and given by $G = \nu e^2/h$.

In this appendix, we wish to explicitly compute the Green's functions for the edge modes in the hydrodynamic regimes described above. In doing so, we shall obtain the temperature dependence for the decay lengths for the neutral modes. The simplest approach is to develop an approximation for the self-energy of the edge modes. However, we find lowest order perturbation theory for the self-energy fails to describe the long wavelength limit of the edge dynamics correctly. Below we will explain the origin of this failure and physically motivate a more accurate description.

Because it is conceptually simpler, we will first focus on the effects of weak impurity scattering in the vicinity of the clean fixed point. The following discussion can easily

be generalized to describe the corresponding physics in the disorder dominated phase.

For simplicity we will consider the specific case of $\nu = 2/(2p+1)$ in which there are only two modes. The generalization to other hierarchical quantum Hall states is straightforward. In Sec. II C, we showed that these two modes may be described in terms of an edge charge density $\partial_x \phi_\rho$ and a single neutral density, $\partial_x \phi_\sigma$ (where we have defined $\phi_\sigma = \Phi_1$). The total action can be written,

$$S = S_0 + S_1 + S_{\text{random}} + \int dx d\tau (\eta_\rho \phi_\rho + \eta_\sigma \phi_\sigma) \ . \quad \text{(B1)}$$

Here

$$S_0 + S_1 = \int dx d\tau \frac{1}{4\pi} \left[\frac{1}{\nu} \partial_x \phi_\rho (i\partial_\tau + v_\rho \partial_x) \phi_\rho \right.$$
$$\left. - \partial_x \phi_\sigma (i\partial_\tau - v_\sigma \partial_x) \phi_\sigma + 2 v_{\text{int}} \partial_x \phi_\rho \partial_x \phi_\sigma \right] \quad \text{(B2)}$$

describes the clean edge and

$$S_{\text{random}} = \int dx d\tau [\xi(x) e^{i\sqrt{2}\phi_\sigma} + \text{c.c.}] \quad \text{(B3)}$$

is a weak perturbation, which describes random impurity scattering between the two channels. As usual, we take $\xi(x)$ to be δ correlated with variance W. η_ρ and η_σ are source terms which may be used to generate Green's functions.

In the absence of interchannel tunneling, the retarded Green's functions

$$G^{0R}_{ab}(x,t) = \langle [\phi_a(x,\tau), \phi_b(0,0)] \rangle \theta(t), \quad \text{(B4)}$$

with $a, b = \rho, \sigma$, may be determined from (B2) by analytic continuation $i\omega_n \to \omega$,

$$G^{0R}_{ab}(q,\omega_n) = 2\pi \begin{pmatrix} \frac{1}{\nu} q(\omega - v_\rho q) & v_{\text{int}} q^2 \\ v_{\text{int}} q^2 & -q(\omega + v_\sigma q) \end{pmatrix}^{-1} . \quad \text{(B5)}$$

To analyze the effects of the random tunneling, we begin by evaluating the self-energy to leading order in W. Since S_{random} only involves ϕ_σ, the only nonzero element of the self-energy matrix is $\Sigma_{\sigma\sigma}$. Evaluating the diagrams shown in Fig. 5 gives

$$\Sigma^{(1)}_{\sigma\sigma}(q,\omega_n) = W \int_0^\beta d\tau (e^{i\omega_n \tau} - 1) P(\tau), \quad \text{(B6)}$$

where

$$P(\tau) = \langle T[e^{i\sqrt{2}\phi_\sigma(\tau)} e^{-i\sqrt{2}\phi_\sigma(0)}] \rangle$$
$$\propto \left[\frac{\pi/\beta}{\sin(\pi\tau/\beta)} \right]^{2\Delta} . \quad \text{(B7)}$$

Here Δ is the scaling dimension of $\exp i\sqrt{2}\phi_\sigma$. Equations (B6) and (B7) are identical to the formula for the current-current correlation function of a point contact connecting two Luttinger liquids, which is related to the conductance of the point contact. We may thus use the results of Ref. 26 to analytically continue to real time and evaluate the retarded self-energy

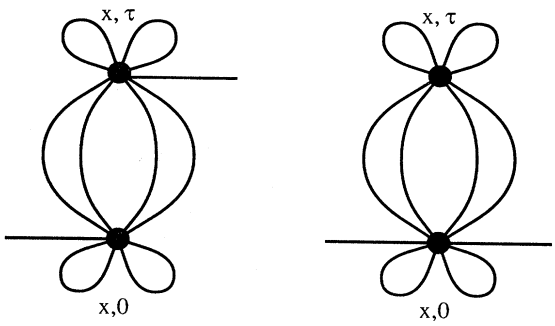

FIG. 5. Diagrams for the self-energy of the Greens function in (B4). The solid circles represent the tunneling operator (B3). The solid lines represent the bare propagator for ϕ_σ, $G^0_{\sigma\sigma}$. A sum over all possible combinations of these lines is implied.

$$\Sigma^{(1)R}_{\sigma\sigma}(q,\omega) = \frac{i\omega}{2\pi\ell}, \quad \text{(B8)}$$

where

$$\ell^{-1} \propto W T^{2\Delta - 2}. \quad \text{(B9)}$$

Below we will interpret ℓ as a mean free path for interchannel scattering. Unfortunately, this leading order approximation to the self-energy does not correctly describe the long wavelength physics of an edge. In particular, it predicts the existence of low-frequency modes, which are inconsistent with the hydrodynamic arguments presented above.

In order to understand the origin of this failure and to physically motivate a way to correct it, it is useful to analyze the Heisenberg equations of motion satisfied by the operators ϕ_ρ and ϕ_σ. These may be derived from (B2) and (B3), and take the form

$$\frac{1}{2\pi} \left[\frac{1}{\nu} (\partial_t + v_\rho \partial_x) \partial_x \phi_\rho + v_{\text{int}} \partial_x^2 \phi_\sigma \right] = \eta_\rho \ , \quad \text{(B10)}$$

$$\frac{1}{2\pi} \left[(-\partial_t + v_\sigma \partial_x) \partial_x \phi_\sigma + v_{\text{int}} \partial_x^2 \phi_\rho \right] = I_\perp + \eta_\sigma, \quad \text{(B11)}$$

where $I_\perp$ is an interchannel tunneling operator given by

$$I_\perp = -i[\xi(x) e^{i\sqrt{2}\phi_\sigma} - \text{c.c.}]. \quad \text{(B12)}$$

In the absence of interchannel tunneling, the propagation of the densities $\partial_x \phi_\rho$ and $\partial_x \phi_\sigma$ is described by the left-hand side of (B10) and (B11). In this case, there will be two eigenmodes, which move at different velocities and are in general linear combinations of ϕ_ρ and ϕ_σ.

The $I_\perp$ in (B12) describes the effect of interchannel tunneling. During a tunneling event, a unit of charge is transferred between the channels. From (B10) we see that this has no immediate effect on the total electric

charge density, $\partial_x\phi_\rho$. However, (B11) shows that a well localized spike of integrated weight 2π is added to the neutral density $\partial_x\phi_\sigma$, which in effect measures the charge difference between the two channels. Equivalently, a soliton is created, in which ϕ_σ winds by 2π.

A linear approximation for the equations of motion may be derived from the self-energy for ϕ_σ in (B8). In particular, Dyson's equation $G^{-1} = G_0^{-1} - \Sigma$ with Σ in (B8) is equivalent to Eqs. (B10) and (B11), with $I_\perp$ replaced by

$$I_\perp^{(1)} = \frac{1}{\ell}\dot{\phi}_\sigma. \tag{B13}$$

This approximation makes physical sense if we identify $\dot{\phi}_\sigma(x)$, via a Josephson-like relation, with the voltage difference between the two channels at point x. Then (B13) is simply a statement of Ohm's law for the tunneling current at x.

However, there is a subtle problem with the interpretation of $\dot{\phi}_\sigma$ as a voltage drop, which can be seen from (B10) and (B11). Let us suppose that at x_1, far away from $x = 0$, an electron tunnels between the two channels at time $t = 0$. Then, according to (B10), there is a δ-function "glitch" in $\dot{\phi}_\sigma(x = 0)$ at time $t = 0$. This occurs because the tunneling event introduces a soliton in ϕ_σ at $x = x_1$, which forces $\phi_\sigma(x = 0)$ to jump by 2π. But this glitch in $\dot{\phi}_\sigma(x = 0)$ cannot correspond to a voltage glitch at $x = 0$ since it must take a finite time for the signal to propagate there. The origin of this discrepancy is the fact that ϕ_σ is an *angular* variable, so that a sudden jump by 2π should have no effect at all. There will be a voltage glitch at $x = 0$ only when the soliton in ϕ_σ (which has a small but finite spatial extent set by the cutoff) propagates through $x = 0$.

Clearly, inclusion of 2π glitches in $\dot{\phi}_\sigma$ in the expression for $I_\perp^{(1)}$ is not physically correct, and is an artifact of the lowest order approximation for the self-energy. We may correct this situation by replacing Eq. (B13) with a modified approximation for the tunneling current, which has the same physical content in terms of Ohm's law, but does not include the 2π glitches in the voltage. We thus substitute $\dot{\phi}_\sigma$ from (B11) into (B13), but then explicitly remove the term from (B11) involving $I_\perp$, which only gives the 2π glitches. We thereby obtain

$$I_\perp^{(2)} = \frac{1}{2\pi\ell}\left(v_\sigma\partial_x\phi_\sigma + v_{\rm int}\partial_x\phi_\rho + \frac{2\pi}{\partial_x}\eta_\sigma\right). \tag{B14}$$

Using the equations of motion with this modified tunneling, including the source terms, we can derive a new approximation for the Green's functions,

$$G_{ab}(q,\omega) = 2\pi\begin{pmatrix} \frac{1}{\nu}q(\omega - v_\rho q) & v_{\rm int}q^2 \\ v_{\rm int}q^2 & -q\left(\frac{\omega}{1-i(q\ell)^{-1}} + v_\sigma q\right)\end{pmatrix}^{-1}. \tag{B15}$$

This corresponds to a neutral mode self-energy

$$\Sigma_{\sigma\sigma}^{(2)}(q,\omega) = \frac{i\omega}{2\pi\ell}\frac{1}{1-i(q\ell)^{-1}}. \tag{B16}$$

To leading order in W (or ℓ^{-1}) $\Sigma_{\sigma\sigma}^{(1)}$ and $\Sigma_{\sigma\sigma}^{(2)}$ are equivalent. However, (B8) breaks down when $q\ell < 1$. In order to describe correctly the long wavelength limit, it is essential to use the modified self-energy (B16).

The validity of this approximation, which we have motivated physically, may be checked in two ways. First, it is clear from (B16) that terms in the self-energy at higher orders in W are singular in the $q \to 0$ limit. We may verify this explicitly by considering the self-energy to order W^2. This involves the expectation value of a product of four of the tunneling operators in (B3). In evaluating this self-energy, care must be taken to subtract off the terms in the expectation value, which are one particle reducible, and hence already accounted for by the leading order term in Σ. The resulting term contains precisely the required singularity, $\omega/(2\pi\ell^2 q)$. Evidently, the approximation (B16) corresponds to summing a class of diagrams, which corresponds to a geometric series in W/q.

An additional nontrivial check of the validity of (B16) is available when $v_{\rm int} = 0$ in (B2). In this case, as shown in Sec. III B, the neutral sector may be solved exactly by mapping onto chiral fermions. We have checked that the ensemble averaged Green's function $G_{\sigma\sigma}$ calculated from this exact solution agrees with the form in (B16).

From (B15) we see that for $W = 0$ there are two propagating modes and, using the results of Appendix A, the conductance is nonuniversal and given by (2.19). In contrast, for any finite W, in the limit $q \ll W^{-1}$, there is only a single propagating mode $\omega = (v_\rho - v_{\rm int}^2/v_\sigma)q$. This reflects the fact that at finite temperatures, when there is interchannel tunneling present, only the total charge is conserved, so that there is a single propagating mode. Moreover, it may be explicitly verified from (B15) that the conductance is given by the quantized value $G = \nu e^2/h$.

We now consider the analogous calculation in the vicinity of the SU(n) random fixed point. In this case, as argued in Sec. III C, we wish to compute the self-energy for G_1, defined in (3.21), due to the random perturbation v_{12}, which has mean square average W_c and couples to $\partial_x\phi_\rho \exp i\sqrt{2}\chi_1$. The self-energy to leading order in W_c is computed by evaluating the diagrams in Fig. 3. We find

$$\Sigma(q,\omega_n) = W_c\int_0^\beta d\tau(e^{i\omega_n\tau} - 1)P(\tau)\ , \tag{B17}$$

where

$$P(\tau) = \langle T[\partial_x\phi_\rho(\tau)e^{i\chi_1(\tau)}\partial_x\phi_\rho(0)e^{-i\chi_1(0)}]\rangle\ , \tag{B18}$$

$$\propto \left[\frac{\pi/\beta}{\sin(\pi\tau/\beta)}\right]^4. \tag{B19}$$

Upon analytically continuing to real frequency, we thus find

$$\Sigma(q,\omega) = \frac{i\omega}{2\pi\ell_\sigma}\ , \tag{B20}$$

with $\ell_\sigma \propto W_c T^2$. It may again be checked that terms in the self-energy higher order in W_c are singular as $q \to 0$. Using arguments analogous to those presented above, we conclude that to correctly describe the long wavelength physics, we must replace (B20) by

$$\Sigma(q,\omega) = \frac{i\omega}{2\pi\ell_\sigma} \frac{1}{1 - i(q\ell)^{-1}}. \tag{B21}$$

[1] J.M. Luttinger, J. Math. Phys. **15**, 609 (1963).
[2] A. Luther and L.J. Peschel, Phys. Rev. B **9**, 2911 (1974); Phys. Rev. Lett. **32**, 992 (1974); A. Luther and V.J. Emery, *ibid.* **33**, 589 (1974).
[3] J. Solyom, Adv. Phys. **28**, 201 (1970); V.J. Emery, in *Highly Conducting One-Dimensional Solids*, edited by J.T. Devreese (Plenum Press, New York, 1979).
[4] F.D.M. Haldane, J. Phys. C **14**, 2585 (1981); Phys. Rev. Lett. **47**, 1840 (1981).
[5] U. Meirav, M.A. Kastner, M. Heiblum, and S.J. Wind, Phys. Rev. B **40**, 5871 (1989).
[6] G. Timp, in *Mesoscopic Phenomena in Solids*, edited by B. L. Altshuler, P.A. Lee, and R.A. Webb (Elsevier, Amsterdam, 1990).
[7] R. Webb (private communication).
[8] See, for example, C.W.J. Beenakker and H. van Houten, in *Solid State Physics: Advances in Research and Applications*, edited by H. Ehrenreich and D. Turnbull (Academic, New York, 1991), Vol. 44.
[9] X.G. Wen, Phys. Rev. B **43**, 11 025 (1991); Phys. Rev. Lett. **64**, 2206 (1990); Phys. Rev. B **44**, 5708 (1991).
[10] A.H. MacDonald, Phys. Rev. Lett. **64**, 222 (1990); M.D. Johnson and A.H. MacDonald, *ibid.* **67**, 2060 (1991).
[11] K. Moon *et al.*, Phys. Rev. Lett. **71**, 4381 (1993).
[12] See, for example, *The Quantum Hall Effect*, edited by R. Prange and S.M. Girvin (Springer-Verlag, New York, 1990).
[13] B.I. Halperin, Phys. Rev. B **25**, 2185 (1982).
[14] M. Buettiker, Phys. Rev. Lett. **57**, 1761 (1986).
[15] X. Wen (unpublished).
[16] B.W. Alphenaar, P.L. McEuen, R.G. Wheeler, and R.N. Sacks, Phys. Rev. Lett. **64**, 677 (1990).
[17] L.P. Kouwenhoven *et al.*, Phys. Rev. Lett. **64**, 685 (1990).
[18] F. Milliken, C. Umbach, and R. Webb (unpublished).
[19] F.D.M. Haldane, Phys. Rev. Lett. **51**, 605 (1983); B.I. Halperin, *ibid.* **52**, 1583 (1984).
[20] C.L. Kane, M.P.A. Fisher, and J. Polchinski, Phys. Rev. Lett. **72**, 4129 (1994).
[21] J.K. Jain, Phys. Rev. Lett. **63**, 199 (1989).
[22] N. Read, Phys. Rev. Lett. **65**, 1502 (1990).
[23] See, X.G. Wen and A. Zee, Phys. Rev. B **46**, 2290 (1992), and references therein.
[24] S.C. Zhang, T.H. Hansson, and S. Kivelson, Phys. Rev. Lett. **62**, 82 (1989); N. Read, *ibid.* **62**, 86 (1989); S.M. Girvin and A.H. MacDonald, *ibid.* **58**, 1252 (1987).
[25] A long-range Coulomb interaction leads to a wave-vector dependent velocity in (2.7), $v \propto \ln(1/q)$. It can be shown that this will restore the quantization of the conductance in an infinite sample. However, in a finite sample of size L, there will be non-negligible corrections to the quantized conductance, which are of order $\ln^{-2} L/a$, where a is the magnetic length.
[26] C.L. Kane and M.P.A. Fisher, Phys. Rev. B **46**, 15 233 (1992).
[27] J. Frohlich and A. Zee, Nucl. Phys. B **364**, 517 (1991).
[28] R.C. Ashoori, H. Stormer, L. Pfeiffer, K. Baldwin, and K. West, Phys. Rev. B **45**, 3894 (1992).
[29] A similar perturbative RG is described in detail in T. Giamarchi and H. Schulz, Phys. Rev. B **37**, 325 (1988).

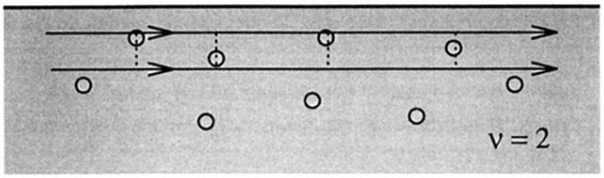

(a)

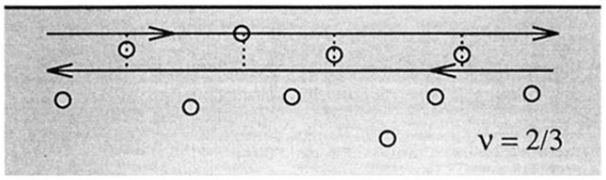

(b)

FIG. 1. Schematic portrait of the edge of a quantum Hall state with two channels. The presence of random impurities, denoted by the small circles, allows for momentum nonconserving scattering between the different channels. When the channels move in the same direction (e.g., $\nu = 2$), as shown in (a), interchannel scattering does not effect the net transmission of the edge. However, when the channels move in opposite directions, as in $\nu = 2/3$, depicted in (b), the backscattering of charge plays a crucial role.